

## Crystal Structure of a New FeP<sub>4</sub> Modification

M. EVAÏN AND R. BREC

*Laboratoire de Chimie des Solides, UER de Chimie, 2, rue de la Houssinière, 44072 Nantes Cédex, France*

AND S. FIECHTER AND H. TRIBUTSCH

*Hahn-Meitner Institut für Kernforschung Bereich Strahlenchemie, Glienicker St. 100, D-1000 Berlin 39 F.R.G., West Germany*

Received October 2, 1986; in revised form January 5, 1987

In addition to monoclinic  $\alpha$ -FeP<sub>4</sub> (space group  $P2_1/c$ ,  $a = 4.619$ ,  $b = 13.670$ ,  $c = 7.002$  Å,  $\beta = 101.48^\circ$ ,  $Z = 6$ ) and orthorhombic  $\beta$ -FeP<sub>4</sub> (space group  $C222_1$ ,  $a = 5.005$ ,  $b = 10.212$ ,  $c = 5.530$  Å,  $Z = 4$ ), a third modification,  $\gamma$ -FeP<sub>4</sub>, has been synthesized and its structure determined from a single-crystal X-ray diffraction study.  $\gamma$ -FeP<sub>4</sub> crystallizes in monoclinic symmetry (space group  $C2/c$ ,  $a = 5.0543(7)$ ,  $b = 10.407(2)$ ,  $c = 11.069(2)$  Å,  $\beta = 91.14(1)^\circ$ ,  $Z = 8$ ). The structure refinement was conducted with 560 unique structure factors yielding a final  $R$  value of 0.026, 49 variables being taken into account. Like the other  $MP_4$  phases, the cations are octahedrally coordinated, and the phosphorous atoms are tetrahedrally surrounded by Fe and P atoms. From atomic bond considerations and ionic radii calculations, a low-spin  $d^6$  configuration is inferred for  $\gamma$ -FeP<sub>4</sub>, and no Fe-Fe bond is found, in agreement with conclusions drawn for  $\alpha$ - and  $\beta$ -FeP<sub>4</sub>. The  $\gamma$ -FeP<sub>4</sub> structure, which can be written as the sequence of planes  $p'o'po$ ,  $p'o'po$ , . . . in the Rühl and Jeitschko symbolism, can be described as constituted of infinite zigzagging chains of (FeP<sub>6</sub>) octahedra sharing only edges. Three such octahedra constitute the linear units of the phase, compared to two and four in CrP<sub>4</sub> and 6-MnP<sub>4</sub>. Interatomic distances found in  $\gamma$ -FeP<sub>4</sub> are identical, within error, to those of the two other iron tetrphosphite modifications. © 1987 Academic Press, Inc.

### Introduction

It has been recently shown that semiconducting transition metal phosphides could be promising materials for optoelectronics and solar energy conversion (1). New syntheses carried out in the iron-phosphorus system led recently to the preparation of a new iron tetrphosphide  $\gamma$ -FeP<sub>4</sub> (2). Preliminary X-ray study indicates that the phase crystallizes with monoclinic symmetry (2) ( $C2/c$  space group), with the following powder spectra refined cell parameters:  $a =$

$5.0543(7)$ ,  $b = 10.407(2)$ ,  $c = 11.069(2)$  Å,  $\beta = 91.14(1)^\circ$ ,  $V = 582.1(3)$  Å<sup>3</sup>,  $Z = 8$ . This paper describes the structure determination of  $\gamma$ -FeP<sub>4</sub> and compares the crystal array of this new phase with that of the two other  $\alpha$ - and  $\beta$ -FeP<sub>4</sub> iron tetrphosphides and some  $MP_4$  transition metal compounds.

### Experimental

To obtain  $\gamma$ -FeP<sub>4</sub> single crystals, the following preparation procedure was used (2).

H<sub>2</sub>-reduced iron powder (60-mesh Ventron m5N) and red phosphorus (Hoechst t6N) in the ratio 1:4 were heated in evacuated (10<sup>-5</sup> mbar) and sealed quartz ampoules (diameter = 28 mm; length = 450 mm) in the presence of bromine (0.1 mg/cm<sup>3</sup>). The red phosphorus was kept at 800 K and the iron powder at 1000 K for 30 days. Crystals as large as 1 mm were obtained. Semiquantitative microprobe analysis performed on single crystals indicated the new phase to be a phosphorus-rich iron compound and the crystal structure determination was done assuming a FeP<sub>4</sub> stoichiometric composition. Subsequent successful structure refinement completely confirmed that assumption (see below). Microscopic observations of  $\gamma$ -FeP<sub>4</sub> crystals clearly showed a systematic twinning of the samples. Since the study of that behavior was not in the scope of the present work, we systematically tried to separate the twinned crystals mechanically in order to obtain a single-crystal sample. After many attempts, this was finally achieved. The symmetry and parameters were determined on a CAD4 diffractometer. Because the crystal did not show any well-formed face, and because of the low absorption factor (70.4 cm<sup>-1</sup>), no absorption correction was made. Table I gathers the main crystallographic and refinement data related to the structure determination.

### Structure Refinement

Programs used belonged to the SDP-PLUS package (1982 version) distributed by ENRAF-NONIUS and written by Frenz (3). Iron atomic positions were deduced from the Patterson map. A series of Fourier and Fourier difference maps helped introduce the remaining atoms. The refinement by a full-matrix least-squares method using scattering factors for neutral atoms corrected for anomalous dispersion and with isotropic temperature factors gave the

TABLE I  
 $\gamma$ -FeP<sub>4</sub> CRYSTALLOGRAPHIC DATA AND PARAMETERS  
OF THE X-RAY DATA COLLECTION AND  
REFINEMENT

Physical, crystallographic, and analytical data
Formula: FeP <sub>4</sub> ; molecular weight: 179.74
Crystal symmetry: monoclinic; space group: C2/c
Cell parameters (293 K):
$a = 5.0543(7)$ Å; $b = 10.407(2)$ Å; $c = 11.069(2)$ Å
$\beta = 91.14(1)^\circ$
$V = 582.1(3)$ Å <sup>3</sup> , $Z = 8$
Density: $\rho_{\text{cal}} = 4.102$
Absorption factor: $\mu(\lambda\text{MoK}\alpha)$ , 70.4 cm <sup>-1</sup>
Crystal size: $\approx 0.020 \times 0.020 \times 0.020$ mm <sup>3</sup>
Data collection
Temperature: 293 K; radiation: MoK $\alpha$
Monochromator: oriented graphite (002); scan mode: $\omega/2\theta$
Recording angle range: 5–30°; scan angle: 0.85 + 0.35 tan $\theta$
Value determining the scan speed:
SIGPRE: 0.85; SIGMA: 0.05; VPRE: 20°/min; $T_{\text{max}} = 60$ sec
Standard reflection: 030, $\bar{1}2\bar{1}$ , $\bar{1}25$ ; periodicity: 3600 sec
Refinement conditions
Utilized reflections: 560 with $I > 3\sigma(I)$
Refined parameters: 49
Reliability factors: $R = \Sigma F_o  -  F_c /\Sigma F_o $
$R_w = [\Sigma_w( F_o  -  F_c )^2/wF_o^2]^{1/2}$
Refinement results
$R = 0.026$ , $R_w = 0.031$
Extinction coefficient: $E_c = 0.37(3) \times 10^{-5}$
Difference Fourier maximum peak intensity; 0.6(1) e <sup>-</sup> /Å <sup>3</sup>

reliability factor value of  $R = 0.040$  and  $R_w = 0.052$ . Introduction of anisotropic temperature factors led then to  $R = 0.026$  and  $R_w = 0.031$ , the extinction coefficient being equal to  $0.37(3) \times 10^{-5}$ . Table II lists the final fractional coordinates of the six independent atoms of the cell and their temperature factors.<sup>1</sup>

<sup>1</sup> See NAPS document No. 04470 for 3 pages of observed and calculated structure factors. Order from ASIS/NAPS. Microfiche Publications, P.O. Box 3513, Grand Central Station, New York, NY 10163. Remit in

TABLE II  
POSITIONAL PARAMETERS<sup>a</sup> AND THEIR ESTIMATED STANDARD DEVIATIONS  
AND REFINED TEMPERATURE FACTOR EXPRESSIONS<sup>b</sup>

Atom	Site	X	Y	Z	$B_{eq}$ (Å <sup>2</sup> )
Fe(1)	4( <i>d</i> )	$\frac{1}{4}$	$\frac{1}{4}$	$\frac{1}{2}$	0.24(1)
Fe(2)	4( <i>e</i> )	0	0.07601(8)	$\frac{1}{4}$	0.22(1)
P(1)	8( <i>f</i> )	0.2997(2)	0.2328(1)	0.2921(1)	0.34(2)
P(2)	8( <i>f</i> )	0.2001(2)	0.4275(1)	0.21573(9)	0.32(2)
P(3)	8( <i>f</i> )	0.0396(2)	0.0926(1)	0.04951(9)	0.32(2)
P(4)	8( <i>f</i> )	0.0608(2)	0.3973(1)	0.02394(9)	0.31(2)

Atom	$B_{11}$	$B_{22}$	$B_{33}$	$B_{12}$	$B_{13}$	$B_{23}$
Fe(1)	0.0021(3)	0.00012(6)	0.00091(5)	0.000(2)	0.000(2)	-0.00005(9)
Fe(2)	0.0019(2)	0.00018(6)	0.00080(5)	0	0.0000(2)	0
P(1)	0.0036(3)	0.00034(7)	0.00103(6)	-0.0002(3)	-0.0004(2)	0.0001(1)
P(2)	0.0024(3)	0.00048(7)	0.00106(6)	-0.0004(3)	0.0000(2)	-0.0000(1)
P(3)	0.0026(3)	0.00045(7)	0.00101(6)	0.0005(3)	0.0003(2)	-0.0001(1)
P(4)	0.0027(3)	0.00045(7)	0.00096(6)	-0.0005(3)	0.0000(2)	-0.0001(1)

<sup>a</sup> Anisotropically refined atoms are given in the form of the isotropic equivalent thermal parameter, defined as,

$$B_{eq} = \frac{1}{3} \sum_i \sum_j B_{ij} a_i a_j.$$

<sup>b</sup> The form of the anisotropic thermal parameter is  $\exp[-(\beta_{11}h^2 + \beta_{22}k^2 + \beta_{33}l^2 + \beta_{12}hk + \beta_{13}hl + \beta_{23}kl)]$ .

## Structural Results and Discussion

Table III gathers the main interatomic distances and angles encountered in the  $\gamma$ -FeP<sub>4</sub> structure, which is shown in two different projections in Figs. 1 and 2. The iron atoms are approximately octahedrally surrounded by phosphorus atoms and the phosphorus atoms are tetrahedrally coordinated, half of them by two metal and two pnictogen atoms and the other half by one metal and three pnictogen atoms. The phos-

phorus anions form two-dimensional sheets of condensed puckered ten-member rings.

There exist essentially two ways to describe the TX<sub>4</sub> compounds (*T* = transition metal, *X*, = P, As). The first one analyzes the puckered two-dimensional network  $T_nX_{4n}$  of the structural stacking and is applicable to  $\eta$ -MnP<sub>4</sub>, CrP<sub>4</sub>, and  $\beta$ -FeP<sub>4</sub>. The second one studies the various connections occurring between (TX<sub>6</sub>) octahedra and consequently the associated pnictogen network. Since  $\gamma$ -FeP<sub>4</sub> can be described either way, two structural descriptions are given below.

Although presenting a purely tridimensional character,  $\gamma$ -FeP<sub>4</sub> can also be described as resulting from the stacking of Fe<sub>n</sub>P<sub>4n</sub> sheets made of [FeP<sub>4</sub>] pentagons and [Fe<sub>2</sub>P<sub>4</sub>] hexagons (Fig. 3). Four such slabs Fe<sub>n</sub>P<sub>4n</sub>, having only slight differences in an-

advance \$4.00 for microfiche copy or for photocopy, \$7.75 up to 20 pages plus \$3.30 for each additional page. All orders must be prepaid. Institutions and Organizations may order by purchase order. However, there is a billing and handling charge for this service of \$15. Foreign orders add \$4.50 for postage and handling, for the first 20 pages, and \$1.00 for additional 10 pages of material, \$1.50 for postage of any microfiche orders.

TABLE III  
 MAIN INTERATOMIC DISTANCES (Å) AND ANGLES (°) IN (FeP<sub>6</sub>), (P<sub>3</sub>Fe<sub>2</sub>), AND (P<sub>4</sub>Fe)  
 POLYHEDRA OF  $\gamma$ -FeP<sub>4</sub> (ESD AND NUMBER OF BONDS AND ANGLES BETWEEN  
 BRACKETS)

Fe(1)–Fe(2)	3.520(1)		
P(1)	2.326(1) (×2)	P(1) –Fe(1)–P(3)	77.63(3) (×2), 102.37(4) (×2)
P(3)	2.257(1) (×2)	P(1) –Fe(1)–P(4)	88.58(3) (×2), 91.42(3) (×2)
P(4)	2.207(1) (×2)	P(3) –Fe(1)–P(4)	89.00(4) (×2), 91.00(4) (×2)
Fe(2)–P(1)	2.268(1) (×2)	P(1) –Fe(2)–P(1)	88.06(6) (×1)
P(2)	2.193(1) (×2)	P(1) –Fe(2)–P(3)	79.22(4) (×2)
P(3)	2.238(1) (×2)	P(2) –Fe(2)–P(3)	98.70(4) (×2)
		P(2) –Fe(2)–P(3)	87.56(4) (×2)
		P(1) –Fe(2)–P(2)	90.82(4) (×2)
		P(1) –Fe(2)–P(3)	94.37(4) (×2)
		P(2) –Fe(2)–P(2)	90.38(6) (×1)
Mean $d_{\text{Fe-P}} = 2.248$			
P(1)–Fe(1)	2.326(1)	Fe(1)–P(1) –Fe(2)	100.03(4)
Fe(2)	2.268(1)	Fe(1)–P(1) –P(2)	105.95(5)
P(1)	2.244(2)	P(2) –P(1) –P(1)	121.26(4)
P(2)	2.248(1)	Fe(1)–P(1) –P(1)	121.72(7)
		Fe(2)–P(1) –P(2)	115.25(5)
		P(1) –P(1) –P(2)	92.37(4)
P(2)–Fe(2)	2.193(1)	Fe(2)–P(2) –P(1)	114.88(5)
P(1)	2.248(1)	Fe(2)–P(2) –P(2)	125.77(4)
P(2)	2.174(2)	Fe(2)–P(2) –P(4)	117.73(4)
P(4)	2.245(1)	P(1) –P(2) –P(2)	94.14(4)
		P(1) –P(2) –P(4)	107.06(5)
		P(2) –P(2) –P(4)	93.01(6)
P(3)–Fe(1)	2.257(1)	Fe(1)–P(3) –Fe(2)	103.11(4)
Fe(2)	2.238(1)	Fe(1)–P(3) –P(3)	113.24(7)
P(3)	2.249(2)	Fe(1)–P(3) –P(4)	118.22(5)
P(4)	2.193(1)	Fe(2)–P(3) –P(3)	113.48(7)
		Fe(2)–P(3) –P(4)	118.11(5)
		P(3) –P(3) –P(4)	90.99(6)
P(4)–Fe(1)	2.207(1)	Fe(1)–P(4) –P(2)	114.85(4)
P(2)	2.245(1)	Fe(1)–P(4) –P(3)	130.32(5)
P(3)	2.193(1)	Fe(1)–P(4) –P(4)	115.72(6)
P(4)	2.283(2)	P(2) –P(4) –P(3)	93.96(5)
		P(2) –P(4) –P(4)	99.60(6)
		P(3) –P(4) –P(4)	96.61(6)
Mean $d_{\text{P-P}} = 2.232$			

gles and interatomic distances, are needed to constitute the basic cell. Using Rühl and Jeitschko symbolism (5),  $\gamma$ -FeP<sub>4</sub> can be described as the sequence of planes p'o'po, p'o'p. . . . This is to be compared to the

stacking sequence of the five other MP<sub>4</sub> structures for which such a symbolism can be used. They are CrP<sub>4</sub> (oo', oo', . . .), 2-MnP<sub>4</sub> (pp, pp, . . .), 6-MnP<sub>4</sub> (ppop'p'o', ppop'p'o', . . .), 8-MnP<sub>4</sub> (pppp, p-p-p-p,



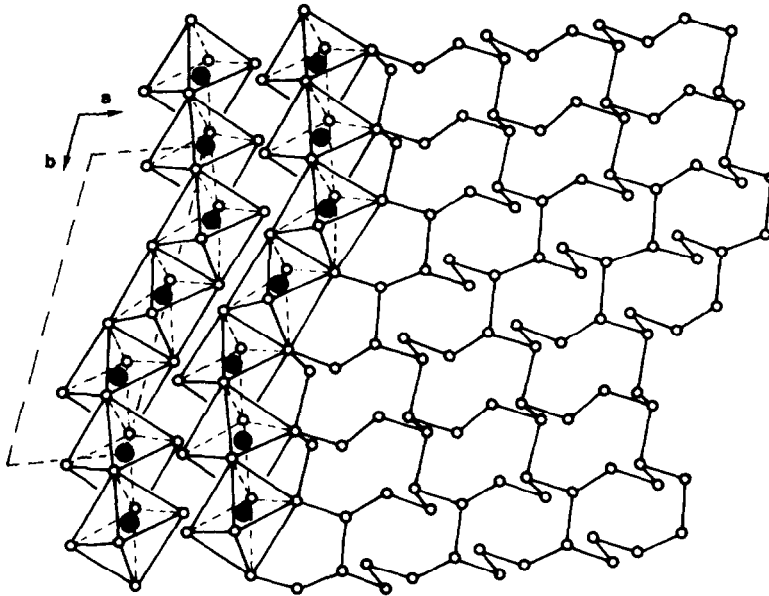


FIG. 2. Perspective drawing of  $\gamma\text{-FeP}_4$  structure (ORTEP) showing the edge-sharing octahedra and their linear arrangement of  $[\text{FeP}_6]_3$  units.

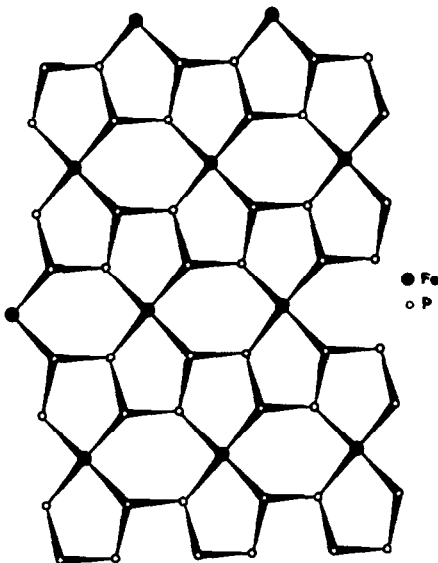


FIG. 3. The puckered sheet, made of  $(\text{Fe}_2\text{P}_4)$  hexagons and  $(\text{FeP}_4)$  pentagons, considered as a building plane of  $\gamma\text{-FeP}_4$ .

If one takes into account two valence electrons for each Fe–P and P–P bond and if one attributes these electrons to the phosphorus polyanion of the structure, a formal charge of +2 is found for iron (8). As demonstrated for the  $\alpha\text{-FeP}_4$  modification (9), iron can be assumed to have, in  $\gamma\text{-FeP}_4$ , a low-spin  $d^6$  configuration and hence the phase is diamagnetic. This would imply unpaired iron cations, and indeed the shortest  $\text{Fe}^{2+}\text{--Fe}^{2+}$  distance is  $3.520(1)$  Å, too long for any intercationic link. The structure keeps the iron ions well separated through the elongation of the  $\text{Fe}(1)\text{--P--Fe}(2)$  angles between the  $[\text{FeP}_6]$  octahedra (see Fig. 1), inducing strong distortion in the structure (Table III). This structure feature was first pointed out by Jeitschko and Braun (8) in  $\alpha\text{-FeP}_4$ .

Further evidence of the iron electronic configuration can also be deduced from the interatomic distances. If one considers the mean Fe–P bond lengths of the three  $\text{FeP}_4$  structures, very similar values are observed, implying the same electronic ar-

TABLE IV  
OBSERVED MEAN METAL-PHOSPHORUS DISTANCES  
IN SOME FIRST-ROW TRANSITION METAL  
TETRAPHOSPHIDES<sup>a</sup>

Compounds	Atomic distances and radii			
	Mean $d_{M-P}$ (Å)	$r_{M^{2+}}$ (Å)	$r_{M^{2+}}$ (Å)	
			Low spin	High spin
CrP <sub>4</sub>	2.336	0.70	0.73	0.80
2-MnP <sub>4</sub>	2.273	0.63	0.67	0.83
6-MnP <sub>4</sub>	2.275	0.63		
8-MnP <sub>4</sub>	2.282	0.64		
$\alpha$ -FeP <sub>4</sub>	2.259	0.62	0.61	0.78
$\beta$ -FeP <sub>4</sub>	2.249	0.61		
$\gamma$ -FeP <sub>4</sub>	2.248	0.61		

<sup>a</sup> Cationic radii were calculated using  $r_P = 1.64$  Å (see text) and compared to that of the same cations in low-spin and high-spin configurations as found in halogenides and chalcogenides (from (10)).

rangement for Fe<sup>2+</sup> (Table IV). Considering a low-spin cationic radius of 0.61 Å for Fe<sup>2+</sup> as given by Shannon and Prewitt (10), an ionic radius of 1.64 Å can be calculated for phosphorus. This latter value yields radii of 0.63 and 0.70 Å, respectively, for Mn<sup>2+</sup> and Cr<sup>2+</sup> in MnP<sub>4</sub> and CrP<sub>4</sub> (Table IV), compared with the values of 0.67 and 0.73 Å for the same ions in low-spin configuration in chalcogenides according to the above reference. All these results are self-consistent and indicate the structure homogeneity of the three FeP<sub>4</sub> compounds as well as that of the MP<sub>4</sub> family ( $M$  = first-row transition metal). They are in agreement with bonding considerations developed by Jeitschko *et al.* (4, 5, 8, 11).

### Conclusion

The new monoclinic  $\gamma$ -FeP<sub>4</sub> compound presents a structure based on edge-sharing (FeP<sub>6</sub>) octahedra. From that point of view, it resembles other tetraphosphides of first-row transition metals that are also built in a similar way, namely CrP<sub>4</sub>, 2-MnP<sub>4</sub>, and 6-

MnP<sub>4</sub>.  $\gamma$ -FeP<sub>4</sub> differs from  $\alpha$ - and  $\beta$ -FeP<sub>4</sub>, which are built through corner sharing in the latter and through corner and edge sharing in the former. As far as bonding is concerned, however,  $\gamma$ -FeP<sub>4</sub> looks very much like the two other iron tetraphosphide compounds with isolated iron ions Fe<sup>2+</sup> in the low-spin configuration ( $t_{2g}^6 e_g^0$ ), implying diamagnetic behavior. This feature constitutes an important difference between the MnP<sub>4</sub> and CrP<sub>4</sub> compounds, for instance, in which metal-metal bonds are observed between adjacent octahedra. As found before, this property is related to the cation  $t_{2g}$  orbital filling state since, in the case of the FeP<sub>4</sub> phases, Fe<sup>2+</sup> in  $t_{2g}^6 e_g^0$  configuration cannot exchange Fe-Fe bonds through the octahedral edges.  $\gamma$ -FeP<sub>4</sub> structure supports and conclusions of previous studies made on related materials and polymorphs and provides a new example of polyhedral combination in the tetraphosphide family.

### References

1. H. TRIBUTSCH, in "Modern Aspects of Electrochemistry" (J.O'M. Bockris, Ed.), Vol. 14, Chap. 4, Pergamon, New York (1986).
2. S. FEICHTER, H. TRIBUTSCH, M. EVAIN, AND R. BREC, *Mater. Res. Bull.* **22**, 543-549 (1987).
3. B. FRENZ, "Enraf-Nonius, Structure Determination Package," Delft Univ. Press, Delft, Netherlands (1982).
4. W. JEITSCHKO AND P. C. DONOHUE, *Acta Crystallogr., Sect. B* **28**, 1893-1898 (1972).
5. R. RÜHL AND W. JEITSCHKO, *Acta Crystallogr., Sect. B* **37**, 39-44 (1981).
6. W. JEITSCHKO, R. RÜHL, U. KRIEGER, AND C. HEIDEN, *Mater. Res. Bull.* **15**, 1755-1762 (1980).
7. M. SUGITANI, N. KINOMURA, M. KOIZUMI, AND S. KUME, *J. Solid State Chem.* **26**, 195-201 (1978).
8. W. JEITSCHKO AND D. J. BRAUN, *Acta Crystallogr., Sect. B* **34**, 3196-3201 (1978).
9. F. GRANJEAN, A. GERARD, U. KRIEGER, C. HEIDEN, D. J. BRAUN, AND W. JEITSCHKO, *Solid State Commun.* **33**, 261-264 (1980).
10. R. D. SHANNON AND C. T. PREWITT, *Acta Crystallogr., Sect. B* **25**, 925 (1969).
11. W. JEITSCHKO AND P. C. DONOHUE, *Acta Crystallogr., Sect. B* **31**, 574-580 (1975).